Supporting information

Label-free visualization of heterogeneities and defects in metal-organic frameworks using nonlinear optics

Mathias Wolf,[a] Kenji Hirai,[b] Shuichi Toyouchi,[a] Eduard Fron,[a] Wannes Peeters,[a] Steven De Feyter[a] and Hiroshi Uji-i*[a,b]*

a. Department of Chemistry, KU Leuven, Celestijnenlaan 200F, 3001 Heverlee, Belgium.

b. Research Institute for Electronic Science (RIES), Hokkaido University, N20W10, Kita ward, Sapporo, 001-0020 Hokkaido, Japan

Corresponding Author * E-mail: hirai@es.hokudai.ac.jp, hiroshi.ujii@kuleuven.be

1. Experimental:

Synthesis of metal organic frameworks (MOFs): Microcrystals of CD-MOF (**1**) was synthesized according to the literature (Nanoscale, 2017,9, 7454-7463). Microcrystals of MOF-177 (**2**) was synthesized according to the literature (J. Mater. Chem., 2007, 17, 3197–3204). Microcrystals of $([(Co(SCN)_2)_3(TPT)_4]_n$ (**3**) was synthesized according to the literature (TPT: 2,4,6-tris(4-pyridyl)-1,3,5-triazine, Nat. Chem., 2010, 2, 780–783). Space groups for the MOFs are **1**: *R*32, **2**: $P\bar{3}1c$, **3**: $Fm\bar{3}m$.

Introduction of C_{60} into MOFs: As-synthesized crystals of **1**, **2** and **3** were immersed into a saturated toluene solution of fullerene C_{60} (10 mL) at room temperature. The suspension was heated to 60^{o}C in an oven. After 1 day, the supernatant was removed by decantation, another 10 mL of saturated fullerene solution was added to the residue, and the resulting suspension was again allowed to stand at 60 ºC. After 1 week with six solution-replacement cycles, the inclusion complex was obtained (Nat. Chem., 2010, 2, 780–783). MOFs accommodating C_{60} fullerene are denoted as **1**$\supset C_{60}$, **2**$\supset C_{60}$ and **3**$\supset C_{60}$. Characterization: X-ray diffraction (XRD) measurements were carried out with SmartLab, Rigaku. The microcrystals of **1**, **2** and **3** were observed by a desktop scanning electron microscope (SEM, Phenom Pro, Phenom-World).

Confocal Microscopy: Nonlinear optics (NLO) and Raman measurements were carried out using an inverted optical microscope (Ti-U, Nikon) equipped with a piezoelectric stage (P517.3CL, Physik Instrument).
For NLO experiments, two laser wavelengths were used at 820 nm (Mai Tai HP, Spectra-Physics, 120 fs, 80 MHz) and 1164 nm (Inspire HF 100, Spectra-Physics). The four-wave mixing (FWM) in this study is so-called degenerate-four-wave-mixing (DFWM) meaning two of the three in-going wavelengths are the same. Radiation is generated at:

$$\omega = \omega_1 + \omega_1 - \omega_2 \qquad (1)$$

Raman spectra were recorded using a 785 nm solid-state laser (Excelsior 785, Spectra-Physics). For both measurements, the excitation beams were focused 2 μm above the glass-MOF interface using an objective lens (60x PlanApo, air, NA 0.95, Nikon). The backscattered NLO and Raman signals were corrected by the same objective, and spectra were recorded using a charge-coupled device (CCD) camera (DU920P, Andor) with a spectrograph (iHR320, Horiba). In order to block excitation light, a 750 short-pass (ET750sp, Chroma) and 800 nm long-pass filter (HQ800LP, Chroma) were used for FWM and

Raman, respectively. NLO and Raman signals from out of focus were removed by a pinhole (diameter 100 µm).

Maps were obtained by using AIST software (AIST-NT) for piezo-controlled movement together with Labspec software (Horiba) to collect spectra at every point. For all MOFs, maps were obtained with a pixel size of 200 x 200 nm^2. Accumulation time at every point was 1 second for NLO maps and 4 seconds for Raman maps. All maps are x,y-slices obtained by focusing the two laser beams 2 µm above the glass-MOF interface. Integration time at every point was 1 s and 4 s for NLO and Raman mapping, respectively.

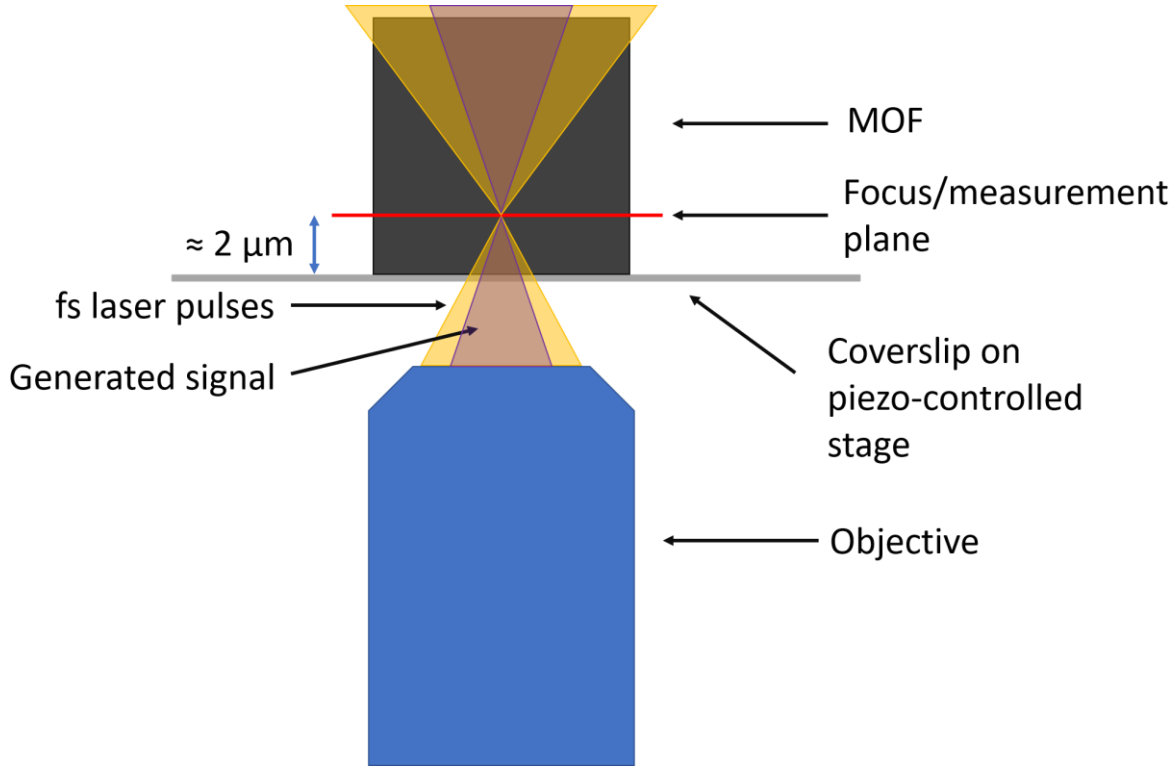

Fig. S1 Schematic of experimental setup. MOFs were put on top of a coverslip which is placed on top of a piezo-controlled stage. The pump beams are focused by an objective below the sample. The generated signal is collected via the same objective. Maps were obtained roughly 2 µm above the coverslip by moving the sample over the objective.

Data analysis was performed using a self-written Python routine. The raw data spectra were smoothed using Savitzky-Golay-filter. The regions of interest were cut out from the spectra. Afterwards a linear background correction was applied. The maximum intensity of peaks was used for mapping.

2. MOF structures

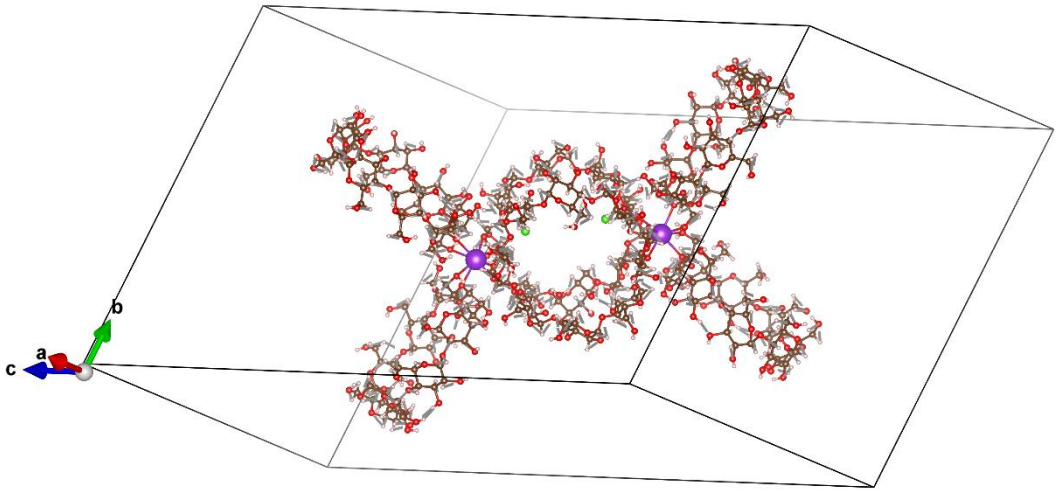

Fig. S2 Structure of **1**. The space group is *R32*. [1,2]

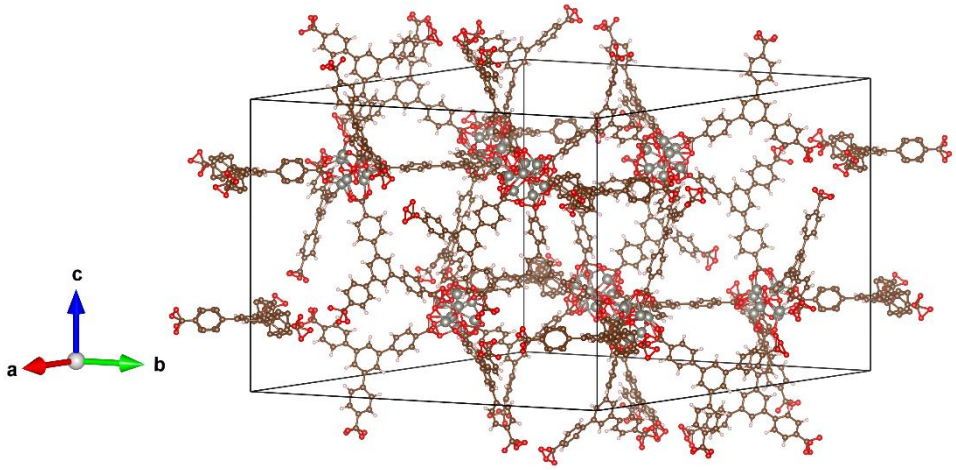

Fig. S3 Structure of **2**. The space group is $P\bar{3}1c$. [1,3]

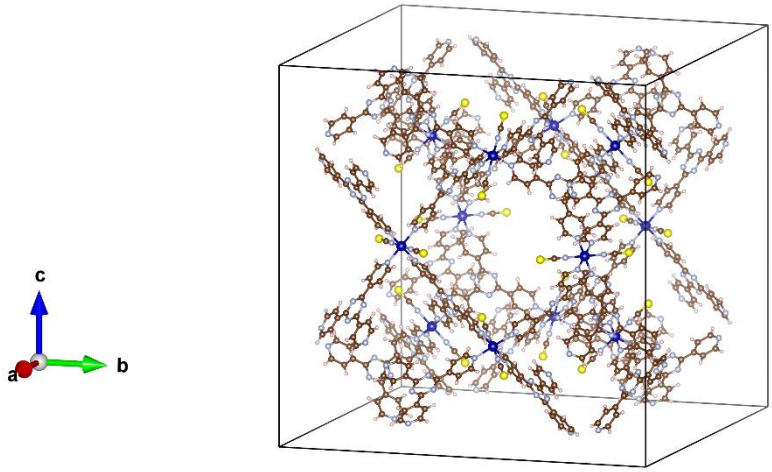

Fig. S4 Structure of **3**. The space group is $Fm\bar{3}m$. [1,4]

3. SEM

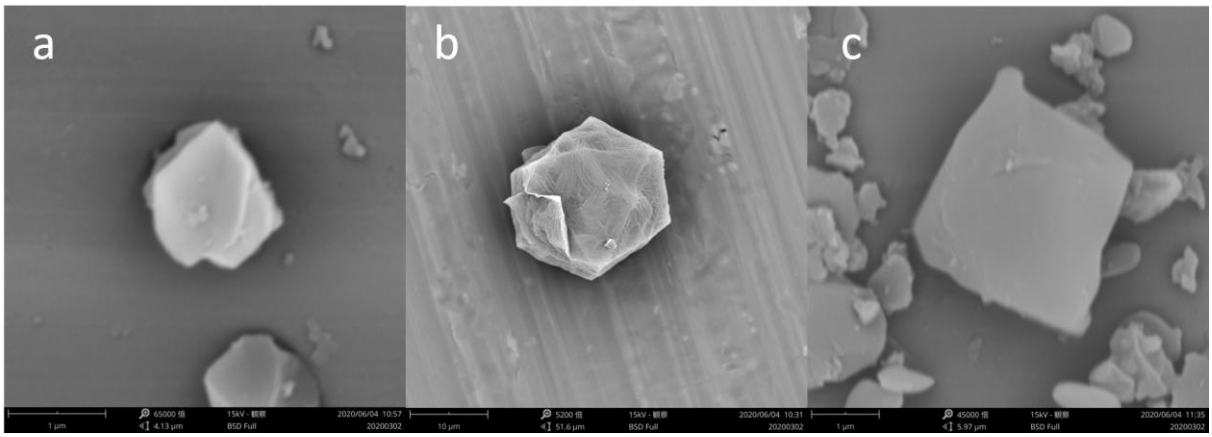

Fig. S5 SEM images from **1** (a), **2** (b) and **3** (c).

4. XRD

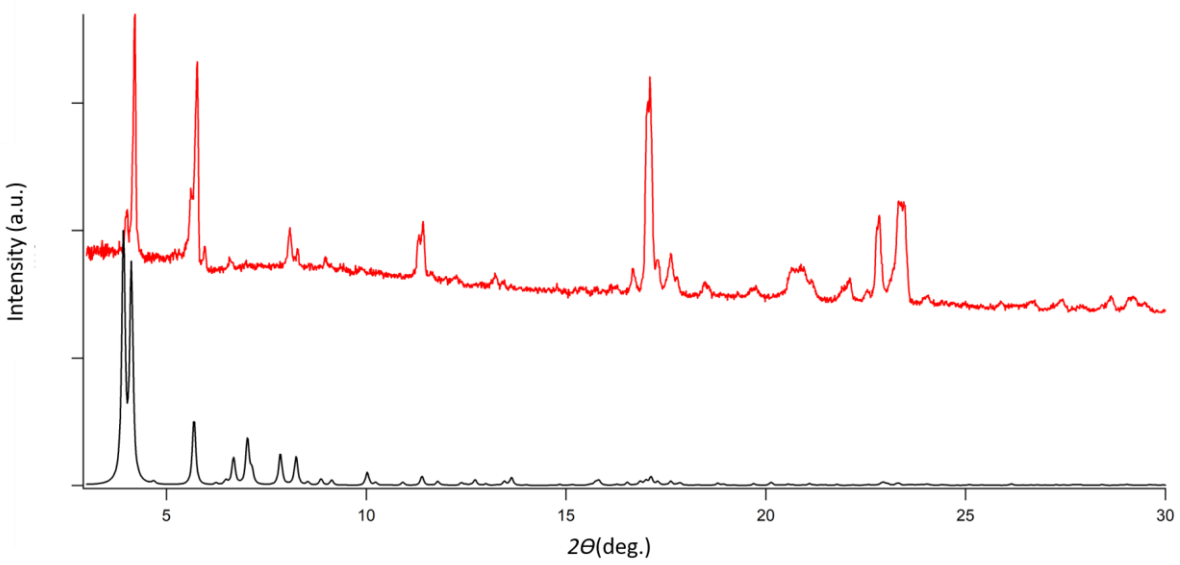

Fig. S6 XRD data obtained from **1** (red) and simulation[2,5] (black).

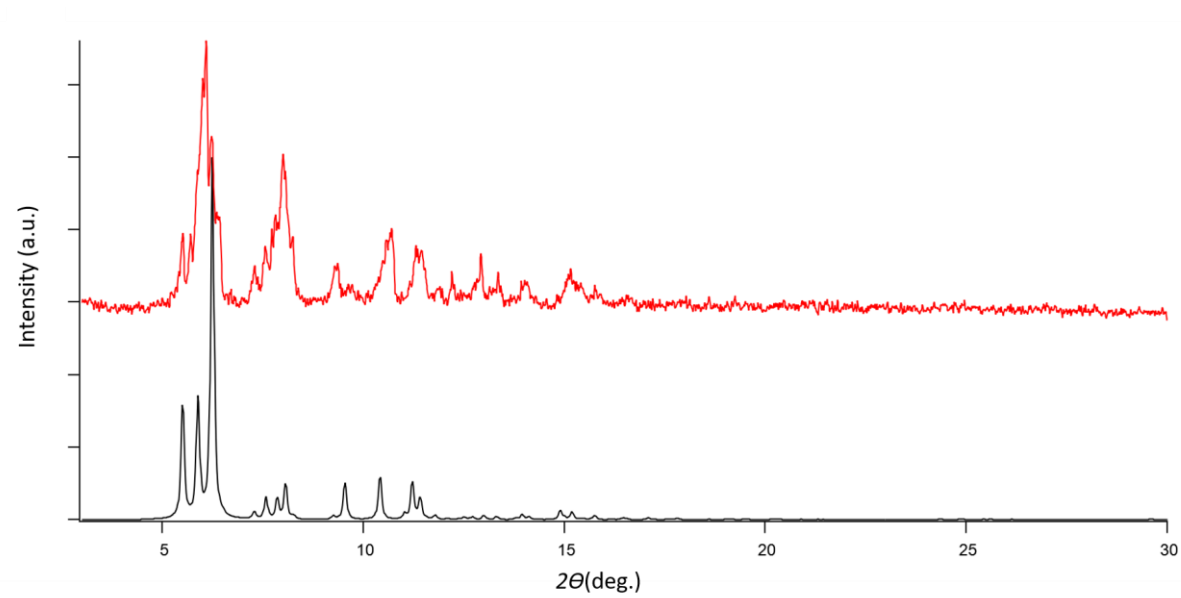

Fig. S7 XRD data obtained from **2** (red) and simulation[3,5] (black).

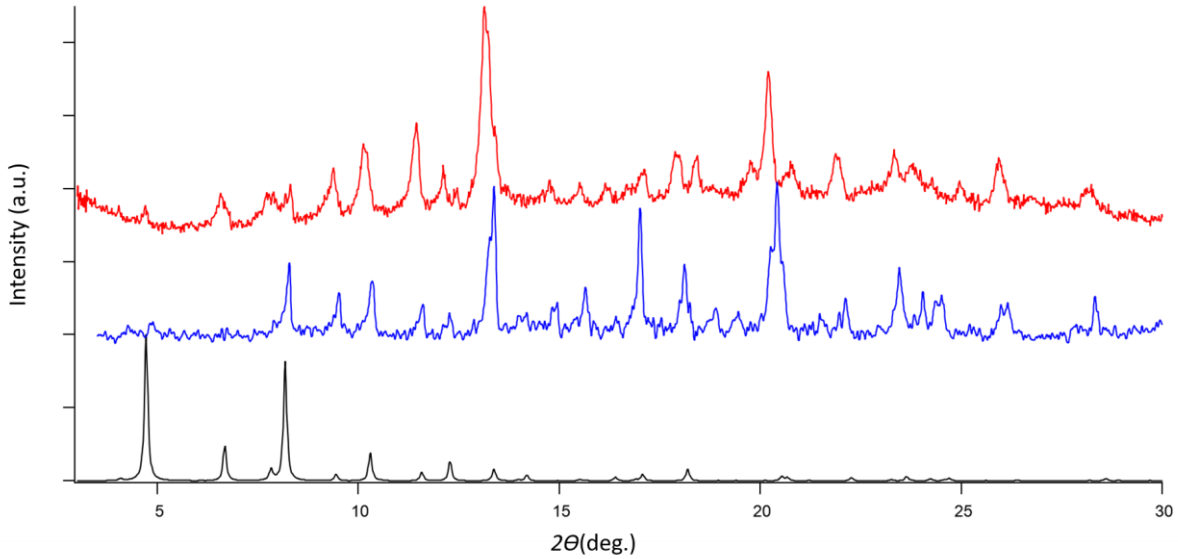

Fig. S8 XRD data obtained from **3** (red), **3**⊃C_{60} (blue) and simulation[4,5] (black).

Fig. S8 shows XRD obtained from **3** and **3**⊃C_{60}. The semi-amorphous state can be seen in red and is characterized by a relatively strong peak at 13° and weak low-angle peaks. After accommodation of C_{60} into the MOF, the data shown in blue is obtained. Compared to the before-mentioned data, it shows stronger low-angle peaks typical for a crystalline structure.

References

1 K. Momma and F. Izumi, *J. Appl. Crystallogr.*, 2011, **44**, 1272
2 K.J. Hartlieb, D.P. Ferris, J.M. Holcroft, I. Kandela, C.L. Stern, M.S. Nassar, Y.Y. Botros and J.F. Stoddart*, Mol. Pharm.,* 2017, **14***, 1831*
3 H.K. Chae, D.Y. Siberio-Pérez, J. Kim, Y. Go, M. Eddaoudi, A.J. Matzger, M. O'Keeffe and O.M. Yaghi*, Nature,* 2004, **427**, 523
4 Y. Inokuma, T. Arai and M. Fujita, *Nat. Chem.*, 2010, **2**, 780
5 C.F. Macrae, I. Sovago, S.J. Cottrell, P.T.A. Galek, P. McCabe, E. Pidcock, M. Platings, G.P. Shields, J.S. Stevens, M. Towler and P.A. Wood, *J. Appl. Cryst.*, 2020, **53**, 226